Testing a random phase approximation for bounded turbulent flow

Mark Ulitsky,* Tim Clark, and Leaf Turner
Theoretical Division, Los Alamos National Laboratory, Mail Stop B216, Los Alamos, New Mexico 87545
(Received 29 September 1998)

Tractable implementation of a spectral closure requires that the modal representation of the energy satisfy a restricted random phase approximation (RRPA). This condition is exactly satisfied when the statistical system is homogeneous and the basis functions are Fourier modes. In this case, the ensemble average of the spectral covariance diagonalizes, i.e., $\langle c(\mathbf{k}_1)c(\mathbf{k}_2)\rangle = \delta(\mathbf{k}_1+\mathbf{k}_2)\langle c(\mathbf{k}_1)c(\mathbf{k}_2)\rangle$, where $c(\mathbf{k},t)$ is a Fourier coefficient in a Galerkin representation of the velocity field. However, for inhomogeneous statistical systems in which the Fourier system is inappropriate, the RRPA requires validation. We use direct numerical simulations (DNSs) of the Navier-Stokes and truncated Euler equations to test the degree to which the RRPA is satisfied when applied to a recent representation due to Turner (LANL Unclassified Report No. LA-UR-96-3257) of a bounded turbulent rectangular channel flow with free slip, stress free walls. It is shown that a *complete* test of the RRPA for a fully inhomogeneous DNS with N^3 grid points actually requires N^3+1 members in the ensemble. The ''randomness'' of the phase can be characterized by a probability density function (PDF) of the modulus of the normalized spectral covariance. Results reveal that for both the Navier-Stokes and Euler systems the PDF does not change in time as the turbulence decays, and that the PDF for the Euler system is virtually identical to the one produced from an ensemble of random fields. This result is consistent with the equipartition of energy for the Euler system, in which the RRPA becomes an exact result rather than an approximation as the number of realizations approaches N^3+1. The *slight* differences observed between the PDF produced from the random fields and the one from the Navier-Stokes system are thus shown to be entirely a result of the presence of a finite viscosity. It is also shown that there is great variation between statistics computed over the ensemble and those for a single realization. [S1063-651X(99)11605-2]

PACS number(s): 47.27.−i, 02.70.Hm

I. INTRODUCTION

Historically, application of the fundamental theories of hydrodynamic turbulence generally have assumed that the ensemble averaged statistics of the turbulent flow under consideration are homogeneous (translation invariant) [1,2]. The motivation for this restricted range of application has been that the assumption of homogeneity tremendously simplifies the mathematical problems attendant to representing the velocity field. Foremost, the assumption of homogeneity permits the use of a Fourier representation of the turbulent flow field, which then leads to further significant simplifications. First, the Fourier representation of a homogeneous signal statistically ''diagonalizes.'' By statistical diagonalization, we mean that when averaged over an ensemble of realizations wherein the ensemble statistics are homogeneous, it trivially can be shown that the Fourier coefficients of the homogeneous signal $\hat{f}(k)$ satisfy

$$\langle \hat{f}(k)\hat{f}(q)\rangle = \langle \hat{f}(k)\hat{f}(q)\rangle \delta(k+q), \tag{1}$$

where $\langle\cdots\rangle$ denotes an ensemble average. Second, the Fourier representation transforms the integrodifferential representation of pressure effects into an algebraic expression, thus greatly simplifying future analysis.

Unfortunately, real turbulence is not homogeneous, even though the pressure effects are still integrodifferential in character. Spectral models based on Fourier representations have been proposed for inhomogeneous turbulence [3,4]. However, these models assume ''approximate homogeneity,'' and thus have limits of validity in real flows. In addition, a Fourier representation for strongly inhomogeneous turbulence is usually not appropriate—the domain is not homogeneous, and furthermore, may not even be periodic. Even so, one still would like a representation in which the pressure can be treated in a straightforward fashion. However, the functional bases appropriate for a particular geometric domain may not diagonalize unless the *ensemble* of realizations of the inhomogeneous field possesses a ''random phase'' property such as that embodied in Eq. (1). The consequences of using a representation that does not diagonalize is that the computational cost for such a representation is prohibitive.

When proposing a functional basis to represent an inhomogeneous signal, one might *assume a priori* that the representation possesses a random phase property such as Eq. (1). We will refer to such an assumption as a restricted random phase approximation (RRPA) [5]. The approximation is restricted in the sense that we are only applying it to the second-order moments. The assumptions necessary to express the higher-order moments will typically be provided by a turbulence theory (e.g., quasinormal assumption [6,7]) and a more general random phase approximation is not necessary. If the RRPA is violated, than one might still propose a diagonalization procedure such as the one presented by Kraichnan [8,9] or Turner [10]. If not, the computational cost of a nondiagonalized representation would render it computationally intractable.

*FAX: 505-665-5926. Electronic address: msu@lanl.gov

The RRPA is an assumption regarding a particular representation of an *ensemble* of realizations. Thus, rigorous testing of the validity of the approximation requires a method of generating a (presumably) finite ensemble that possesses the restricted random phase property [e.g., Eq. (1)], and then time-evolving the individual realizations and testing to what degree the restricted random phase property is satisfied at various times during the evolution.

The choice of ensemble averages, as opposed to temporal or spatial averages is motivated by physical concerns, as well as by pragmatic mathematical considerations. Fundamentally, we wish to produce a theory which will tell us how the statistics of an ensemble of realizations of a system will evolve from a statistically characterizable ensemble of initial states. Pragmatically, the construction of ensemble averages is the most straightforward approach to develop statistical models of inhomogeneous, nonsteady turbulence. In the special cases of time-invariant (stationary) or space-invariant (homogeneous) turbulence, other averages *may* be appropriate. For stationary or homogeneous turbulence, a temporal or spatial average is often substituted for an ensemble average. The justification for such alternatives to ensemble averaging is attributed to an ''ergodic hypothesis'' regarding the turbulence. Such an ergodic hypothesis would require that the statistics of the ensemble of realizations be represented in a single particular realization which may, or may not, be a member of the ensemble. The validity of the ergodic hypothesis for Navier-Stokes turbulence has never been established, and as a result, attempts to compute statistics from a small number of direct numerical simulations of homogeneous turbulence (rather than the full ensemble) should be viewed with caution (see the Appendix).

The goal of the present paper is to show what is required to provide a rigorous determination of the validity of the RRPA using direct numerical simulations of the Navier-Stokes equations for an inhomogeneous turbulent channel flow [5] (described in the next section), and to determine whether a particular Galerkin representation of the velocity field reasonably satisfies some measure of RRPA. The computational task of ''proving'' RRPA is unfortunately beyond the capability of current computing resources, except in the most trivial circumstances. In fact, it will be demonstrated that to completely establish RRPA for this particular representation of the field would require a minimum of N^3+1 members in the ensemble for a grid with N^3 points. We will also show a congruency of the statistics of the decaying channel flow with a system which can be shown analytically to satisfy the RRPA [11,12], namely, the truncated Euler equations represented in the same functional basis. In addition, the implications of RRPA for spectral modeling and for meaningfully comparing simulation results with those of a spectral model for this bounded turbulent flow will be elucidated.

The plan of the paper is as follows. In the next section (Sec. II), we first describe the particular flow geometry as well as the functional decomposition of the flow field that we are studying. In addition, we will introduce the notion of a RRPA in the context of this functional representation. In Sec. III, we describe how we generate an ''ensemble'' of initial conditions which satisfies the RRPA. In Sec. IV we describe the evolution of these states subjected to the dynamics of the Navier-Stokes equations and also to the dynamics of the truncated Euler equations. We demonstrate that the solutions of the Navier-Stokes equations are consistent with an ensemble of states of a system which does satisfy the random phase assumption, e.g., the truncated Euler equations. In Sec. V we present our conclusions.

II. VELOCITY DECOMPOSITION FOR A BOUNDED TURBULENT ''SLAB''

In the second of a series of three papers, Turner [5] rigorously derived a velocity decomposition for an inhomogeneous turbulent flow in terms of a presumably complete set of solenoidal eigenfunctions. The geometry under consideration was that of a rectangular channel with free slip, stress free walls at $y=0$ and $y=L_y$ and with periodic boundary conditions in the x and z directions. The main result from that work was that the velocity field in physical space could be expressed as

$$\mathbf{u}(\mathbf{r},t)=\sum_{\mathbf{k}} c(\mathbf{k},t)\boldsymbol{\Delta}(\mathbf{k},\mathbf{r}), \tag{2}$$

where the summation is over all modes $\mathbf{k}$. The spectral coefficients in a Galerkin representation of the velocity field are $c(\mathbf{k},t)$. The solenoidal basis vectors $\boldsymbol{\Delta}(\mathbf{k},\mathbf{r})$, have components with the following form:

$$\Delta_x=f_x(\mathbf{k})\cos k_y y e^{i(k_x x+k_z z)}, \tag{3}$$

$$\Delta_y=f_y(\mathbf{k})\sin k_y y e^{i(k_x x+k_z z)}, \tag{4}$$

$$\Delta_z=f_z(\mathbf{k})\cos k_y y e^{i(k_x x+k_z z)}. \tag{5}$$

The presence of Fourier modes in the axisymmetric directions and either sine or cosine modes in the inhomogeneous direction will enable a standard pseudospectral method to be used to update the velocity field. More will be said about the numerical updating procedure in a later section. The complex-valued vector $\mathbf{f}$ results from the particular geometry and boundary conditions being considered, and is solely a function of the position vector $\mathbf{k}$, where

$$f_x=\frac{1}{\sqrt{2}}\left[\frac{-k_x k_z+ikk_y}{k\sqrt{k_x^2+k_y^2}}\right], \tag{6}$$

$$f_y=\frac{1}{\sqrt{2}}\left[\frac{kk_x-ik_y k_z}{k\sqrt{k_x^2+k_y^2}}\right], \tag{7}$$

$$f_z=\frac{1}{\sqrt{2}}\frac{\sqrt{k_x^2+k_y^2}}{k}. \tag{8}$$

Here, k refers to the magnitude of $\mathbf{k}$. To contrast this decomposition with one for a box of fluid with periodic boundary conditions, we note that for the latter there would be Fourier modes in all three directions, and $c(\mathbf{k},t)\mathbf{f}(\mathbf{k})$ would be replaced by $\mathbf{u}(\mathbf{k},t)$. Also, in the degenerate case where $k_x=0=k_y$, the solenoidal eigenvectors take on the following simple form:

$$\Delta_x = -\frac{1}{\sqrt{2}} e^{i(k_z z)}, \tag{9}$$

$$\Delta_y = 0 = \Delta_z . \tag{10}$$

For more details about the derivation of this velocity decomposition, the interested reader should refer to Ref. [5].

Before discussing the RRPA, however, it will be useful to list two important properties of $c(\mathbf{k})$:

$$c(-\mathbf{k}) = c^*(\mathbf{k}), \tag{11}$$

$$\langle c(\mathbf{k}) \rangle = 0. \tag{12}$$

Note that the time dependence of the spectral coefficients will no longer be explicitly stated in order to simplify notation. The first property is simply the reality condition, which guarantees that the physical space velocity calculated via Eq. (2) is a real-valued vector field. The second property applies to the ensemble as opposed to a particular realization, and in effect, defines $c(\mathbf{k})$ as a zero-mean fluctuating variable.

The RRPA also applies to the ensemble and takes the form of $\langle c(\mathbf{k}) c^*(\mathbf{p}) \rangle = 0$, unless $\mathbf{p} = \mathbf{k}$. This approximation might superficially resemble that of homogeneity, but in fact, there is no relation between them. For example, consider that even with the RRPA, the y component of the velocity field must vanish at the channel walls in order to satisfy the no-penetration condition at the two boundaries. Thus the flow *cannot* be homogeneous in the y direction. Also, the RRPA is only being applied here to second order moments, whereas homogeneity restricts moments of arbitrary order.

The RRPA enables one to define an ensemble averaged energy spectrum as follows:

$$\hat{E}(\mathbf{k}) \equiv \langle c(\mathbf{k}) c^*(\mathbf{k}) \rangle = 4E(\mathbf{k}). \tag{13}$$

The hat on the energy spectrum is used to distinguish this quantity from the more traditional $E(\mathbf{k})$, which has the property that a sum over all states yields the total kinetic energy per mass. A sum over all states of $\hat{E}(\mathbf{k})$ actually produces *four* times the total kinetic energy per mass.

One should realize that the RRPA does not make reference to any additional statistical-closure–additional-closure assumptions would be necessary if one wished to model (rather than simulate) the temporal evolution of $\hat{E}(\mathbf{k})$. This is precisely the reason why direct numerical simulations (DNS) can be used to test the RRPA, irrespective of the particular closure scheme ultimately chosen for the spectral model. The RRPA is critical from a modeling perspective because the extra dimensionality involved in transporting $\hat{E}(\mathbf{k},\mathbf{p})$ versus $\hat{E}(\mathbf{k})$ is computationally prohibitive. That is, even for a relatively simple spectral model like the eddy damped quasi-normal Markovian model (EDQNM) [13], the number of operations per time step jumps from $O(N^6)$ to $O(N^{12})$ if one does not employ the RRPA while the storage requirements jump from $O(N^3)$ to $O(N^6)$. This large jump in the number of operations and storage requirements clearly shows the difference between a diagonal and nondiagonal representation of the spectral covariance. Since the RRPA will therefore be at the crux of any rigorous computable spectral model for inhomogeneous turbulence, it is imperative that we attempt to check its validity through DNS before constructing models which by necessity, will simply assume its validity *a priori*.

III. GENERATING AN INITIAL ENSEMBLE SATISFYING THE RRPA

For the truncated Euler equations [11], the RRPA assumption is consistent with what one would obtain for second-order correlations in an absolute equilibrium ensemble. For this system, the statistical steady state is one in which the RRPA becomes an exact result instead of an approximation. This result will be helpful when assessing the influence of the Navier-Stokes dynamics on the RRPA, since the Euler system can always provide a lower bound on the error for a given number of realizations. What we first need to determine however, is N_r, the minimum number of realizations necessary to generate an ensemble of initial fields that can be used to test the RRPA.

To answer this question, assume we have a uniform three-dimensional (3D) lattice with N^3 points. For homogeneous turbulence represented by a Fourier series, only $N^3/2$ of these points are independent for a given realization as a result of the reality condition [Eq. (11)]. For the inhomogeneous problem under consideration, the sine and cosine modes lead to $2N$ points being needed in the k_y direction while the Fourier modes contribute N points in the k_x and k_z directions. Again, only half of these points are independent for a particular realization, and so there are actually N^3 independent modes. At each independent mode $\mathbf{k}$ construct the vector $c^{(i)}(\mathbf{k})$, where the vector superscript corresponds to the particular realization in the ensemble and ranges between 1 and N_r (the quantity we are trying to determine). With this ansatz, it is clear that the RRPA can be restated in terms of inner products of complex vectors and is equivalent to finding an orthogonal basis for these vectors. That is,

$$\langle c(\mathbf{k}) c^*(\mathbf{p}) \rangle \equiv \frac{1}{N_r} \sum_{i=1}^{N_r} c^{(i)}(\mathbf{k}) c^{*(i)}(\mathbf{p}) = 0 \quad \text{for} \quad \mathbf{k} \neq \mathbf{p}. \tag{14}$$

The first part of this equation merely defines the ensemble average, while the second part is the assertion made by the RRPA. The constraints imposed by having to simultaneously satisfy the RRPA and the reality condition lead to the expected result that the dimension of each vector must be greater than or equal to the number of vectors in the half-space. It would of course be mathematically impossible to produce an orthogonal basis if the dimension of each vector were smaller than this quantity. Equation (12) provides an additional constraint that must be satisfied for each vector, and thus the final value for N_r, is N^3+1.

Although perhaps not too surprising, it is somewhat disheartening to accept the fact that so many realizations must be performed to test the RRPA in a nontrivial fashion. What is more disconcerting is that even if N^3+1 members are somehow included in the ensemble, there is no guarantee for the Navier-Stokes system that an ensemble of initial conditions that satisfy the RRPA will satisfy the RRPA as the ensemble evolves in time. This is precisely what we are attempting to verify. In fact, even a relatively coarse grid con-

sisting of 32^3 grid points would require the evolution of 32 769 velocity fields to test the RRPA. It is certainly in our best interest to determine what penalty is incurred by including fewer than 32 769 fields in the ensemble.

If we consider the normalized spectral covariance, defined as

$$\chi = \frac{\langle c(\mathbf{k})c^*(\mathbf{p})\rangle}{\sqrt{\langle c(\mathbf{k})c^*(\mathbf{k})\rangle\langle c(\mathbf{p})c^*(\mathbf{p})\rangle}}, \tag{15}$$

then according to the RRPA, this quantity should be zero for any two nonidentical modes. As χ in general will be a complex number, it can be expressed in polar form as $re^{i\theta}$, and the RRPA asserts that we should have a Dirac delta function at $r=0^+$ for all time. However, when the number of realizations is less than N_r, linear dependencies will prevent χ from being zero for some choices of $\mathbf{k}$ and $\mathbf{p}$, and a distribution of χ values will result.

To generate the initial conditions, a Box-Muller algorithm [14] was used to produce Gaussian distributed $[N(0,1)]$ random numbers for each of the $c^{(i)}(\mathbf{k})$ fields. The mean at each mode, $\langle c(\mathbf{k})\rangle$ was then computed and subtracted off, so that the the new values of $c^{(i)}(\mathbf{k})$ satisfied Eq. (12). In performing the Gram-Schmidt orthogonalization procedure, it will be useful to identify both the real and imaginary parts of $c^{(i)}(\mathbf{k})$ and $c^{(i)}(\mathbf{p})$ as follows:

$$c^{(i)}(\mathbf{k}) = a^{(i)} + ib^{(i)} \quad \text{and} \quad c^{(i)}(\mathbf{p}) = d^{(i)} + ie^{(i)}. \tag{16}$$

To enforce both $\langle c(\mathbf{k})c^*(\mathbf{p})\rangle = 0$ and $\langle c(\mathbf{k})c^*(-\mathbf{p})\rangle = 0$ implies that

$$\langle ad\rangle = \langle ae\rangle = \langle bd\rangle = \langle be\rangle = 0. \tag{17}$$

The decorrelation of, say, $\langle ad\rangle$ is accomplished by

$$d^{(i)} = d^{(i)} - \frac{\langle ad\rangle}{\langle aa\rangle} a^{(i)}, \tag{18}$$

where terms on the right-hand side refer to the current value of those variables, while the term on the left-hand side refers to the new values for $d^{(i)}$.

The Gram-Schmidt (GS) algorithm can now be summarized by the following steps. First, map the 3D wave vectors to a 1D scalar so that the GS algorithm only need be applied to 1D lists. This will greatly facilitate decorrelating all the desired modes and also ensure no decorrelated modes will be accidentally recorrelated. Without loss of generality, assume each list contains N elements (e.g., we wish to generate N orthogonal vectors). Next, assume the first member of the ith list is $c^{(i)}(\mathbf{k})$ and then use Eq. (18) (where $d^{(i)}$ is replaced by $b^{(i)}$) to enforce $\langle ab\rangle = 0$. This is necessary to ensure that $\langle c(\mathbf{k})c^*(-\mathbf{k})\rangle = 0$. Then go to the second, third, ..., Nth members of the list and decorrelate the real and imaginary parts of each member from both $a^{(i)}$ and $b^{(i)}$ using Eq. (18). After proceeding through the entire list, adjust the values of $b^{(i)}$ by the following scaling factor:

$$b^{(i)} = b^{(i)} \sqrt{\frac{\langle aa\rangle}{\langle bb\rangle}}, \tag{19}$$

so that $\langle bb\rangle = \langle aa\rangle$. Again, this condition is necessary for $\langle c(\mathbf{k})c^*(-\mathbf{k})\rangle = 0$. Now proceed to the second member of the list and start the procedure again. If there are N vectors in the list, then it will require N passes (with each pass containing one fewer member than the previous) to generate the orthogonal basis.

The fields are then normalized so that the ensemble averaged autocorrelation at each mode is unity [i.e., $\langle c(\mathbf{k})c^*(\mathbf{k})\rangle = 1$]. The spherically ensemble averaged energy spectrum of random numbers $\hat{E}_{\text{rand}}(k)$ was then computed, and the scalar coefficients were modified for the final time by

$$c^{(i)}_{\text{new}}(\mathbf{k}) = c^{(i)}_{\text{old}}(\mathbf{k}) \sqrt{\frac{\hat{E}(k)}{\hat{E}_{\text{rand}}(k)}}, \tag{20}$$

where $\hat{E}(k)$ is the spectrum with the desired scaling. One other important point concerning the initialization procedure is that Eq. (12) is *not* sufficient to guarantee that a mean flow will not develop over time. As shown in Ref. [5], the additional constraint of $\hat{E}(\mathbf{k}) = \hat{E}(\mathbf{k}_-)$ must also be satisfied at $t=0$, where if $\mathbf{k} \equiv (k_x, k_y, k_z)$, then $\mathbf{k}_- \equiv (k_x, -k_y, k_z)$.

IV. NUMERICAL APPROACH

To time-evolve either the Navier-Stokes or truncated Euler equations, the velocity field in the $\mathbf{k}$ space must first be expressed in terms of the spectral coefficients and the solenoidal basis vectors. From Eq. (2), one can use the orthogonality of the basis vectors to derive the following expression for $\mathbf{u}(\mathbf{k})$:

$$u_\alpha(\mathbf{k}) = f_\alpha(\mathbf{k})c(\mathbf{k}) + f_\alpha(\mathbf{k}_-)c(\mathbf{k}_-) \quad \text{for} \quad \alpha = x \text{ or } z,$$

$$u_y(\mathbf{k}) = f_y(\mathbf{k})c(\mathbf{k}) - f_y(\mathbf{k}_-)c(\mathbf{k}_-). \tag{21}$$

Thus, it is seen that the velocity at a particular mode depends not only on quantities evaluated at that mode, but also on quantities evaluated at the reflected mode across the k_y plane. Equation (21) can be simplified slightly by noting that Eqs. (6)–(8) imply $f_i(\mathbf{k}_-) = f_i^*(\mathbf{k})$. A complication results from the fact that for $k_y = 0$, the orthonormality condition on the solenoidal eigenvectors [which include both the trigonometric functions and the geometric vector $\mathbf{f}(\mathbf{k})$] is slightly different from the one which just involves the trigonometric functions. As the DNS will involve only the latter representation, that is,

$$u_\alpha(\mathbf{r},t) = \sum_{\mathbf{k}} u_\alpha(\mathbf{k},t)\cos k_y y e^{i(k_x x + k_z z)} \quad \text{for} \quad \alpha = x \text{ or } z, \tag{22}$$

$$u_y(\mathbf{r},t) = \sum_{\mathbf{k}} u_y(\mathbf{k},t)\sin k_y y e^{i(k_x x + k_z z)}, \tag{23}$$

an extra factor of $\sqrt{2}$ must be applied to the right-hand side of Eq. (21) when $k_y = 0$ to ensure that Parseval's theorem is satisfied.

We will now consider the evolution of three ensembles, each consisting of 17 members. The first ensemble E1 was generated using a Gram-Schmidt procedure to produce a sys-

TABLE I. Ensemble characteristics.

Type	GS	ν	Δt	No. realizations	Scaling of $E(k)$
Navier-Stokes	Yes	0.25	variable	17	$k^4e^{-k^2/2}$
Euler	No	0	fixed	17	k^2
Navier-Stokes	No	0.25	variable	17	$k^4e^{-k^2/2}$

tem that initially satisfied the RRPA. Since only 17 realizations were considered, only 32 modes in each $c^{(i)}(\mathbf{k})$ field (16 modes and their conjugates) were nonzero at $t=0$. Only 3D high-energy containing modes were selected, and the nonlinear advective terms filled in the other modes as the turbulence cascaded to smaller scales and was redistributed by the pressure field. The initial ensemble averaged energy spectrum scaled as $k^4e^{-k^2/2}$ and the 17 velocity fields were evolved using the Navier-Stokes equations. The second ensemble E2 had an ensemble averaged energy spectrum that scaled as k^2 (the scaling for an absolute equilibrium ensemble without helicity) and the initial spectral coefficients were not orthogonalized with the GS procedure. This ensemble was evolved by the truncated Euler equations. E3, the third ensemble, is identical to E1, with the exception that the GS procedure is not applied at $t=0$. These initial conditions are summarized in Table I.

The grid for the three ensembles was fixed at $20\times30\times20$, with dealiazing of the nonlinear terms accomplished by phase shifting in the k_x and k_z directions and a $\frac{2}{3}$ truncation in the k_y direction. The lack of translation invariance in the k_y direction eliminates the phase shift method as a possible choice for removing the aliasing error in the inhomogeneous direction. Second order Runge-Kutta and Adams-Bashforth schemes were used to update the four coupled ordinary differential equations [continuity and Navier-Stokes (NS)-Euler] with an adaptive time step employed for the NS runs and a fixed time step of 1×10^{-4} for the Euler runs. While truncation to a sphere is certainly appropriate for isotropic box turbulence, the rectangular geometry in this problem suggests the use of an ellipsoidal truncation with minor axes dictated by the number of Fourier modes and major axis by the number of sine or cosine modes. Thus, only modes lying within an ellipsoid whose minor axes equal ten and major axis equal twenty were updated. The NS ensembles were run with a kinematic viscosity of $\nu=0.25$ until $t=2.0$, at which time approximately 95% of the initial kinetic energy per mass had been dissipated. For the Euler runs, a length scale can be defined by

$$L=\lim_{n\to\infty}\frac{\int_0^{k_{\max}}k^nE(k)dk}{\int_0^{k_{\max}}k^{n+1}E(k)dk}=\frac{1}{k_{\max}}. \tag{24}$$

if $E(k)$ scales as a power law in k [here $E(k)$ scales as k^2], and a time scale by $\tau=L/u'$, where u' is the rms velocity. The present grid size and ellipsoidal truncation dictate that $k_{\max}=20$, and u' for the Euler system was fixed at $\sqrt{1/3}$. This resulted in a time scale of 8.66×10^{-2} and the Euler system was evolved for approximately 11.5 of these cycle times.

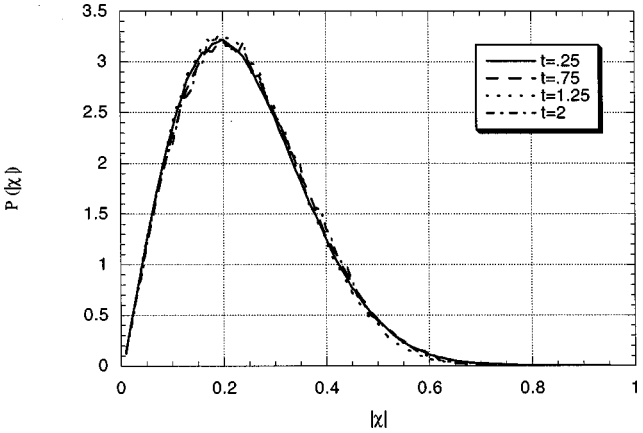

FIG. 1. The time history of the PDFs of $|\chi|$ for the E1 ensemble.

V. RESULTS AND DISCUSSION

A. E1 runs

Figure 1 shows probability density functions (PDFs) of $|\chi|$ at several different times during the E1 run. Recall that at $t=0$, there is a Dirac delta function at $|\chi|=0^+$ as a result of the orthogonalization procedure. Clearly, the effect of the initial condition is quickly lost and a distribution evolves that is stationary in time. Note that ''zero vectors'' are not included in the sample space of the PDF. That is, there is a criterion at each time based on the largest value of the autocorrelation $\langle c(\mathbf{k})c^*(\mathbf{k})\rangle$ among the independent modes. If an autocorrelation at a particular mode is smaller than 10^{-7} times this maximum value, then that vector is discarded from the sample space. Therefore as time progresses in the decaying turbulent system, more vectors will be discarded and the PDF will become slightly noisier. It should also be noted that this maximum autocorrelation value is $O(1)$ at $t=0$.

There are two competing effects occurring to generate the stationary PDF in Fig. 1. One is due to the limited degrees of freedom present as a result of only updating 17 velocity fields (instead of the 12 001 fields necessary for the current grid), which mathematically manifests itself through linear dependencies among most of the modes. The other effect is a result of the nonlinear dynamics of Navier-Stokes equations themselves, which could possibly alter the initial delta function PDF even if enough fields ($\geqslant N_r$) were evolved. To try and separate out these effects, it will be useful to consider how random an ensemble can be when there are not enough degrees of freedom for it to be truly random. To this end, 17 scalar fields of spectral coefficients have been generated using the Box-Muller random number algorithm [14] referred to in the previous section.

Figure 2 shows the PDF of $|\chi|$ produced from the ensemble of random fields with the PDF computed at $t=0.25$ from the Navier-Stokes ensemble. Note that the number of random vectors generated is *identical* to the number of ''nonzero'' vectors present in the Navier-Stokes ensemble. One can conclude from the figure that the apparent effect of

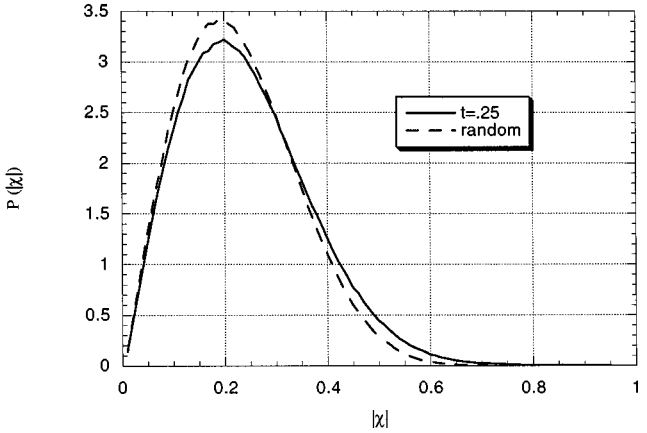

FIG. 2. PDFs of $|\chi|$ for the E1 ensemble at $t=0.25$ and for the ensemble of random fields generated by the Box-Muller algorithm.

the Navier-Stokes dynamics is to keep the spectral coefficients near their most random position possible given the limited number of realizations in the ensemble. If we postulate that the PDF of the Navier-Stokes ensemble will continue to closely mimic that of the PDF from the random ensemble as the number of realizations approaches N_r, then Fig. 3 strongly suggests that the RRPA is a very reasonable assumption. That is, as the number of random fields increases, the PDF progressively approaches a Dirac delta function at $|\chi|=0^+$, which is entirely consistent with the RRPA. Even if the PDF does not become a true delta function as the number of realizations increases, once the number of fields is greater than or equal to N_r, the GS procedure can always be used to produce an orthogonal basis which would then lead exactly to a Dirac delta function PDF at $|\chi|=0^+$.

The PDFs shown in Fig. 1 can be parametrized by $\Delta k \equiv|\mathbf{k}-\mathbf{p}|$. In this way, one can determine whether modes which are closer together exhibit more or less random phase than those possessing larger separation distances in the functional space. These results for E1 are displayed in Fig. 4 for seven ranges of Δk at $t=0.25$, and combined with those from Fig. 1 demonstrate that not only is there no temporal dependence to these PDFs shortly after $t=0$, but neither is there any strong spatial dependence. The ranges in Δk are

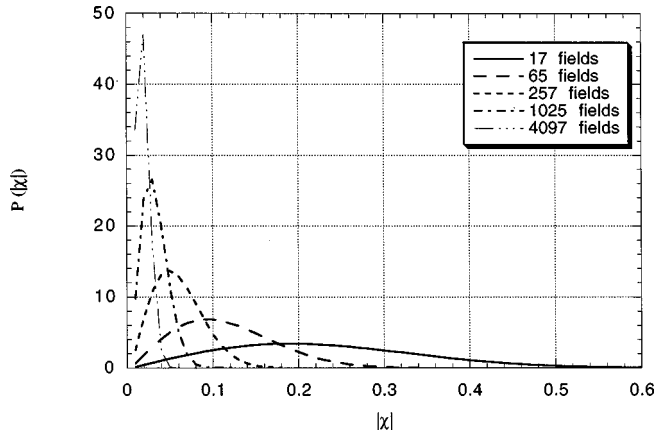

FIG. 3. PDFs of $|\chi|$ for 17, 65, 257, 1025, and 4097 fields of spectral coefficients generated by the Box-Muller algorithm.

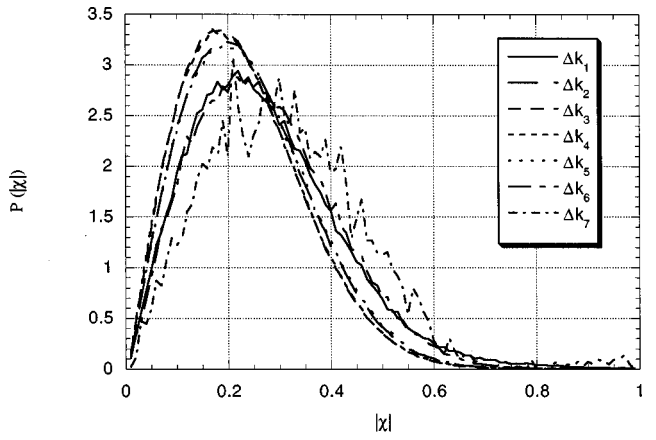

FIG. 4. PDFs of $|\chi|$ for the E1 ensemble at $t=0.25$ parametrized by separation distance in the projected space.

defined as follows (note that the length of the intervals is constant and assumes the value of 3.8):

$$1.0+3.8j\leqslant\Delta k_{j+1}<1.0+3.8(j+1) \quad \text{for} \quad j=0\text{–}5,$$

$$1.0+3.8j\leqslant\Delta k_{j+1}\leqslant1.0+3.8(j+1) \quad \text{for} \quad j=6. \quad (25)$$

Similar results are also obtained for later times.

It is not clear from Fig. 1 which pairs of modes are contributing to the large values of $|\chi|$, however, Eq. (21) suggests that a correlation might exist between modes $\mathbf{k}$ and $\mathbf{k}_-$. The results of this hypothesis are presented in Fig. 5, which shows the PDF of $|\chi|$ at $t=0.25$, 0.75, and 1.25, where only cross correlations between $\mathbf{k}$ and $\mathbf{k}_-$ modes are included in the sample space. It is readily observed that the PDF at $t=0.25$ is almost the mirror image of the one that results for that instant in time when all cross correlations are considered. At later times, however, the PDFs become more uniform. Although it would not be computationally prohibitive to modify the RRPA to include the ensemble correlation between $c(\mathbf{k})$ and $c(\mathbf{k}_-)$, it is not really clear at this point whether a non-vanishing correlation truly exists or is simply an artifact of the limited number of realizations or the spe-

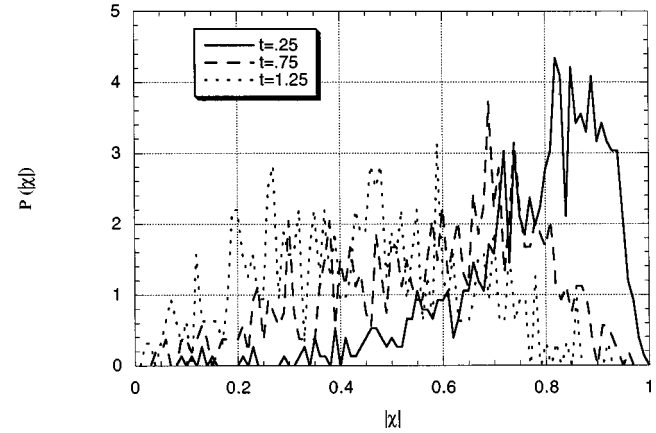

FIG. 5. PDFs for the E1 ensemble at $t=0.25$, 0.75, and 1.25, where only cross correlations between the $\mathbf{k}$ and $\mathbf{k}_-$ modes are considered.

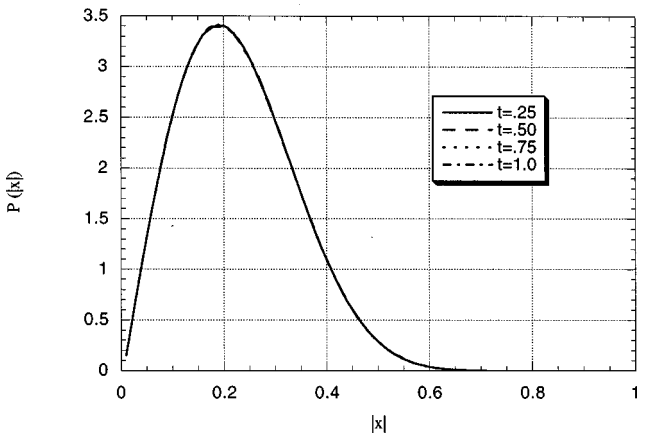

FIG. 6. The time history of the PDFs of $|\chi|$ for the E2 ensemble.

cific initial conditions for the E1 ensemble. This issue will be explored in more detail by examining similar PDFs for the E2 and E3 ensembles.

B. E2 runs

The principal motivation for performing the Euler runs is the analytic result that the RRPA becomes exact for the equilibrium ensemble if the number of realizations is greater than or equal to N_r. When viscosity is present, the resulting non-Hamiltonian nature of the Navier-Stokes equations precludes this analytic result. Of course, since only 17 members are included in the present ensemble, we know that the RRPA cannot hold and a distribution of $|\chi|$ values (other than a Dirac delta function at $|\chi|=0^+$) is inevitable. These PDFs are displayed in Fig. 6 and are strikingly similar to those from E1. Not only are they stationary, but they also seem to possess a nearly identical shape as those from the NS run. These PDFs do not become noisier as the ensemble evolves, as the total energy in the Euler system is conserved and our sample space remains constant in time.

Just as for the NS system, we can construct a PDF with the same number of samples as those in Fig. 6 that utilizes the Box-Muller algorithm to generate the ensemble of spectral coefficients. A comparison between this PDF and the one

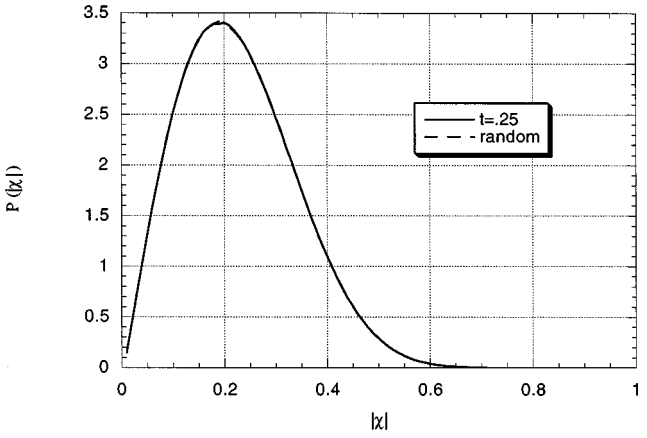

FIG. 7. PDFs of $|\chi|$ for the E2 ensemble at $t=0.25$ and for the ensemble of random fields generated by the Box-Muller algorithm.

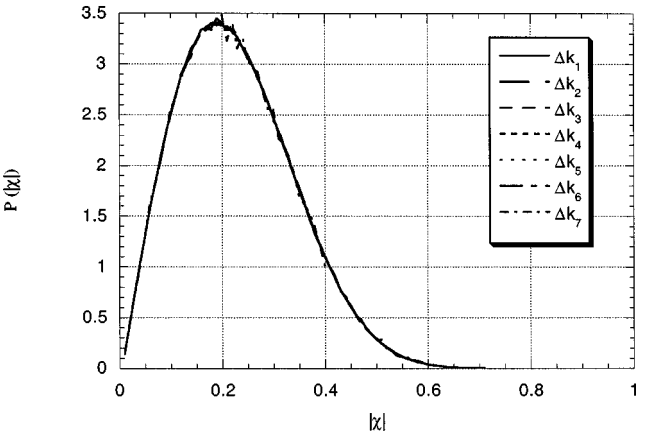

FIG. 8. PDFs of $|\chi|$ for the E2 ensemble at $t=0.25$ parametrized by separation distance in the projected space.

from the Euler system is shown in Fig. 7. The curves overlap perfectly, and thus allows us to interpret the slight differences observed between the PDFs in Fig. 2 as purely being the result of a finite viscosity. One can conclude from Fig. 7 that the equipartition of kinetic energy results in spectral coefficients which are in as random a configuration as possible given the limited number of degrees of freedom in the ensemble.

Figure 8 shows the PDFs of $|\chi|$ for the Euler system at $t=0.25$ parametrized by Δk. Here, seven equally spaced ranges of Δk are considered, where

$$1.0+5.3j \leqslant \Delta k_{j+1} < 1.0+5.3(j+1) \quad \text{for} \quad j=0\text{–}5,$$

$$1.0+5.3j \leqslant \Delta k_{j+1} \leqslant 1.0+5.3(j+1) \quad \text{for} \quad j=6. \quad (26)$$

Again, these distributions do not exhibit any changes as we cover the full spectrum of possible separation distances, proving that in the equilibrated Euler system, there is no spatial dependence for the PDFs of the spectral coefficients. This is essentially the same result obtained for the E1 runs and the PDFs show similar behavior at later times.

For the NS system, it appeared at early times that there was a relatively strong correlation between the $\mathbf{k}$ and $\mathbf{k}_-$ modes (see Fig. 5). The same PDFs can be calculated for the

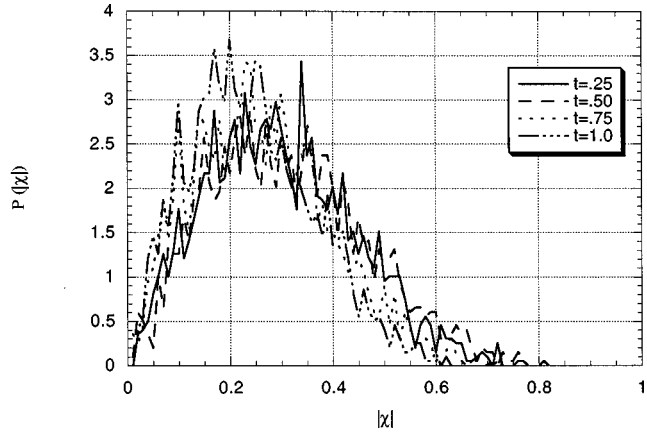

FIG. 9. PDFs for the E2 ensemble at $t=0.25$, 0.50, and 0.75, and 1.0, where only cross correlations between the $\mathbf{k}$ and $\mathbf{k}_-$ modes are considered.

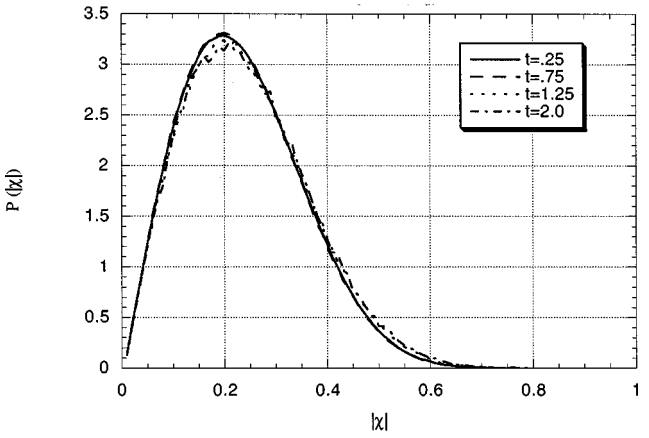

FIG. 10. The time history of the PDFs of $|\chi|$ for the E3 ensemble.

Euler system, and these are displayed in Fig. 9. Note that the lack of smoothness in these PDFs is a natural consequence of the fact that most cross correlations in the ensemble are not between the $\mathbf{k}$ and $\mathbf{k}_-$ modes, and thus the sample space for these PDFs is much smaller than for the PDFs in Fig. 6. Figure 9 shows that at both early and late times, there is no evidence to support a correlation between a mode and its reflected mode across the k_y plane. However, recall that the E1 ensemble was orthogonalized at $t=0$, while the E2 ensemble was not. Therefore, it is not obvious whether the correlations observed at short times for the E1 run are due in part to the initial conditions or are a result of the presence of a finite viscosity. This is the principal motivation behind the E3 runs, which are identical in all respects to the E1 ensemble, but do not employ the GS procedure at $t=0$.

C. E3 runs

Figure 10 shows the time history of the PDFs of $|\chi|$ for the E3 ensemble. Clearly, whether the orthogonalization procedure is applied at $t=0$ does not have any effect on the stationary distribution which quickly evolves. The only difference is the time required to relax into this distribution, which is slightly longer for the E1 ensemble, as it starts off as a

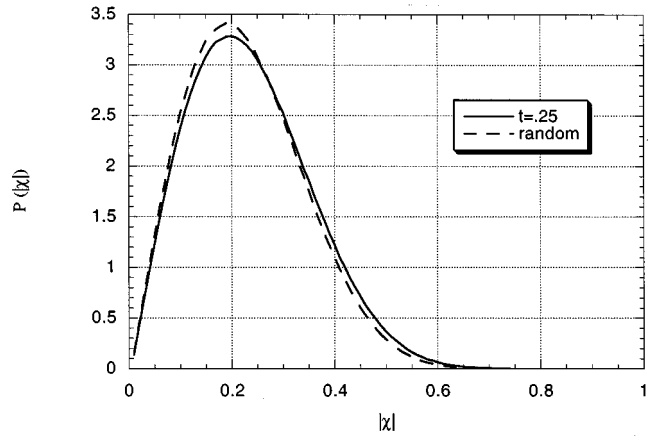

FIG. 11. PDFs of $|\chi|$ for the E3 ensemble at $t=0.25$ and for the ensemble of random fields generated by the Box-Muller algorithm.

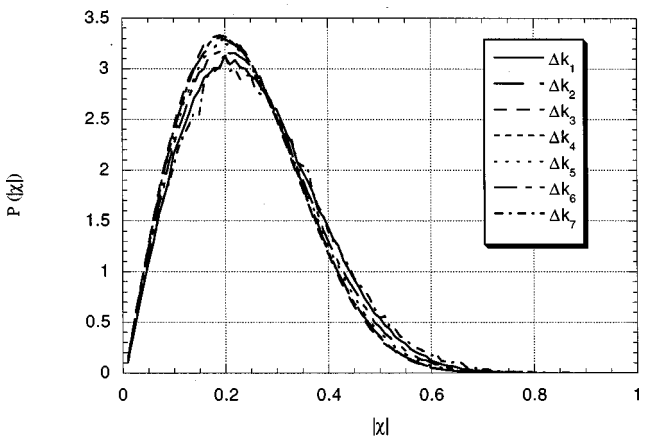

FIG. 12. PDFs of $|\chi|$ at $t=0.25$ parametrized by separation distance in the projected space for the E3 ensemble.

Dirac delta function at $t=0$ (instead of a PDF such as the random curve in Fig. 2). Figure 11 along with Fig. 2 confirm that the minute differences observed between the PDF produced from the 17 random fields and the one produced from the NS system are actually a result of a nonzero viscosity, and not the initial conditions of the two NS ensembles. Figure 12 suggests that just as was previously observed for the E1 ensemble, there is only a weak spatial dependence to the ensemble averaged cross correlations of the spectral coefficients. Here the ranges in Δk are defined as

$$1.0+3.9j \leqslant \Delta k_{j+1} < 1.0+3.9(j+1) \quad \text{for} \quad j=0\text{–}5,$$

$$1.0+3.9j \leqslant \Delta k_{j+1} \leqslant 1.0+3.9(j+1) \quad \text{for} \quad j=6. \quad (27)$$

The major difference between the two NS ensembles is that when the GS procedure is applied, there is a strong tendency for correlations to occur at early times between the $\mathbf{k}$ and $\mathbf{k}_-$ modes. It is readily seen from Fig. 13, however, that the correlation between these two modes is no different from that among any other two modes in the system for the initially nonorthogonalized NS ensemble. This figure suggests that the strong correlations observed in the E1 en-

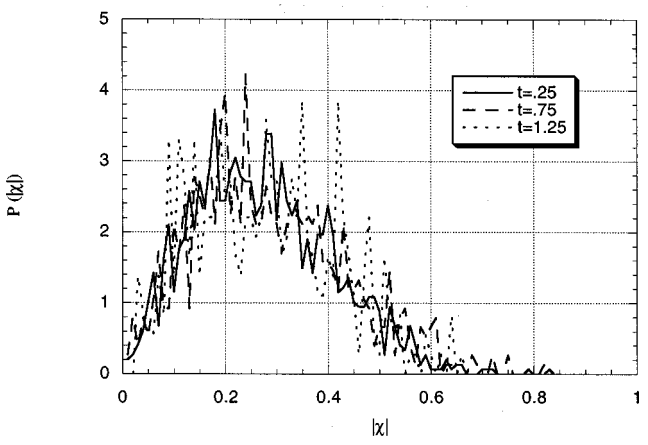

FIG. 13. PDFs for the E3 ensemble at $t=0.25$, 0.75, and 1.25, where only cross correlations between the $\mathbf{k}$ and $\mathbf{k}_-$ modes are considered.

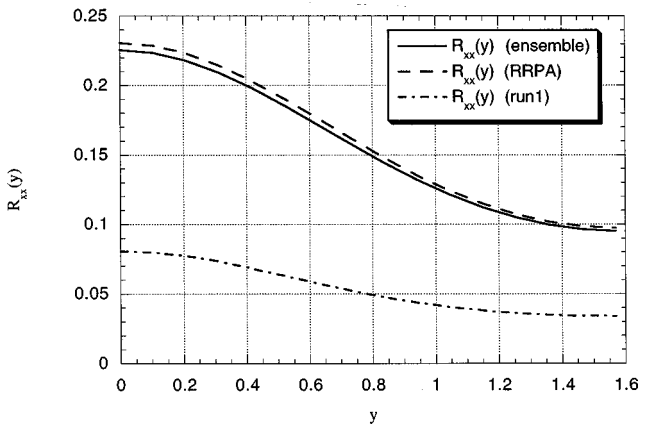

FIG. 14. The *xx* component of the Reynolds stress at $t=2.0$ for the E1 ensemble; a comparison of the ensemble average to that of a single realization as well as to an ensemble that obeys the RRPA.

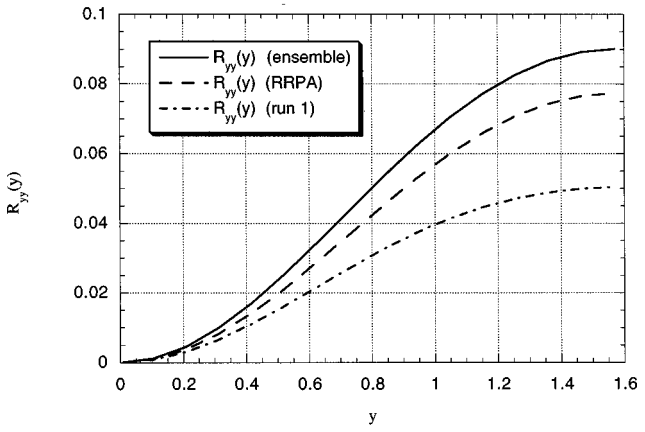

FIG. 15. The *yy* component of the Reynolds stress at $t=2.0$ for the E1 ensemble; a comparison of the ensemble average to that of a single realization as well as to an ensemble that obeys the RRPA.

semble are probably the result of starting with a distribution that is so disparate from the stationary distribution which ultimately evolves. If it were possible to run the E1 ensemble with a much larger number of members in the ensemble, it is unlikely that such strong correlations between the $\mathbf{k}$ and $\mathbf{k}_-$ modes would be observed.

D. Single-point Reynolds stress

Heretofore, we have considered the RRPA only in its broadest sense. That is, we have intentionally not performed spatial integrations in the x and z (periodic) directions. Although the PDFs in Fig. 1 show that most of the cross-correlations between two different modes do not vanish, we can, in effect, eliminate the majority of their nonzero contribution by spatially averaging over all y planes and making use of the orthogonal properties of the Fourier modes. The quantities of interest are the single-point diagonal Reynolds stress components as a function of distance across the channel. In particular, we wish to calculate

$$R_{\alpha\alpha}(y)\equiv\left\langle \int u_\alpha(\mathbf{x})u_\alpha(\mathbf{x})dxdz \right\rangle, \tag{28}$$

where α takes the value of x, y, or z. From an engineering perspective, these are the primary quantities of interest (typically, one would also be interested in pressure-velocity, pressure-strain, and triple velocity correlations). Note that a result of orthogonality is to greatly reduce the number of cross correlations. Here we have that

$$\langle c(\mathbf{k})c^*(\mathbf{p})\rangle=\delta(k_x-p_x)\,\delta(k_z-p_z)\langle c(\mathbf{k})c^*(\mathbf{p})\rangle. \tag{29}$$

Thus, testing the RRPA after spatially averaging over the periodic directions is tantamount to checking that for given values of k_x and k_z, that all the k_y modes are decorrelated from each other over the ensemble.

Figures 14–16 show the diagonal Reynolds stress components for the ensemble of 17 runs along with the same components for a single realization (run 1) at $t=2$ for the E1 ensemble. Also shown for the sake of comparison are the diagonal Reynolds stress components that can be trivially derived from Eq. (2) by assuming the RRPA is valid. These components have the following form:

$$R_{\alpha\alpha,\mathrm{RRPA}}(y)=\frac{1}{2}\sum_{\mathbf{k}} P_{\alpha\alpha}(\mathbf{k})\cos^2(k_y y)\times\langle c(\mathbf{k})c^*(\mathbf{k})\rangle \quad \text{for} \quad \alpha=x \text{ or } z,$$

$$R_{\alpha\alpha,\mathrm{RRPA}}(y)=\frac{1}{2}\sum_{\mathbf{k}} P_{\alpha\alpha}(\mathbf{k})\sin^2(k_y y)\langle c(\mathbf{k})c^*(\mathbf{k})\rangle \quad \text{for} \quad \alpha=y, \tag{30}$$

where $P_{ij}(\mathbf{k})$ is the transverse projection operator defined as

$$P_{ij}(\mathbf{k})=\delta_{ij}-\frac{k_i k_j}{k^2}. \tag{31}$$

Note that the channel actually has a length of π in the y direction, but only values up to the midline are shown (the other halves of the profiles are simply the mirror images of the ones shown in the figures). Again, even if we make no

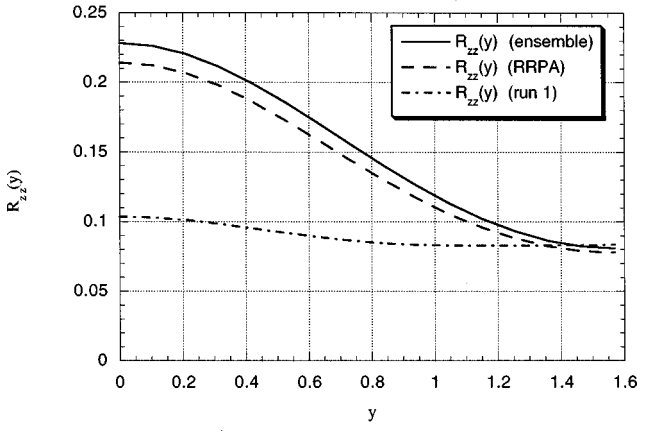

FIG. 16. The *zz* component of the Reynolds stress at $t=2.0$ for the E1 ensemble; a comparison of the ensemble average to that of a single realization as well as to an ensemble that obeys the RRPA.

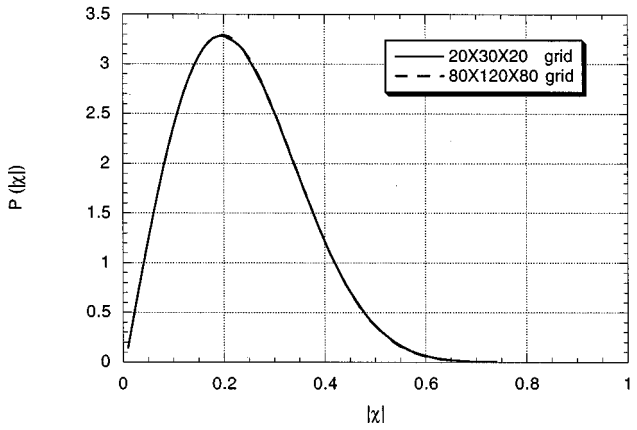

FIG. 17. PDFs of $|\chi|$ showing the effect of increasing the resolution of the E3 ensemble.

assumption about the RRPA, the spatial averaging procedure leads to a result in which the only possible cross correlations are those between the y components in the **k** space. Thus, it should not be too surprising that relatively good agreement is observed between the $R_{\alpha\alpha}(y)$ and $R_{\alpha\alpha,\mathrm{RRPA}}(y)$.

What is rather disturbing is the wide variation observed between a single realization and the entire ensemble. Clearly, it would be very difficult to justify using the statistics obtained from a single run with any fidelity. Note that the only difference between the 17 runs at $t=0$ is the random number seed that goes into the Box-Muller algorithm. In a future study, we will start with an ensemble having initial conditions that satisfy Eq. (29) rather than the more general definition of the RRPA. The advantage of this procedure is that the ensemble will only require $O(N)$ members instead of $O(N^3)$, and thus a complete set of fields can be evolved. We will also focus on homogeneous turbulence and any differences that result from spatially averaging and assuming ergodicity vs computing statistics from an ensemble average.

E. Effect of resolution on the RRPA

Due to the large number of runs that result from evolving three ensembles, all results to this point have been for grids that were $20\times30\times20$. One can question whether the addition of more modes would significantly change the results presented thus far. To this end, a series of 17 runs was performed (equivalent to the E3 ensemble) at a resolution of $80\times120\times80$. The initial velocity fields for this ensemble were identical to those for the E3 ensemble and the higher modes in k space were set to zero. The kinematic viscosity was then decreased so that $k_{\max}\eta$ ($\eta\equiv$Kolmogorov scale) was the same for both runs. Figure 17 shows the PDF of $|\chi|$ at comparable times in the evolution of the two ensembles (the more resolved ensenble needed to be run approximately twice as long to reach the same stage of decay as the lower resolved ensemble), and it is clear that the PDFs are virtually indistinguishable from each other. This is entirely consistent with the PDFs generated from the random fields, where it was observed that the sensitive parameter was the size of the ensemble, and not the number of points in each ensemble. Thus, we can conclude that as one goes to more resolved grids, the proportion of off-diagonal products of spectral coefficients having a particular value of $|\chi|$ remains virtually unchanged. This also suggests that one does not have to evolve a larger number of velocity fields at a higher resolution to get the same percentage error in the statistics that one sees for the lower resolved runs. That is, it is sufficient to evolve identical sized ensembles, since the PDF is essentially independent of the number of grid points.

F. Implications for spectral modeling

The literature is replete with comparisons of single- and two-point statistics between DNS and spectral models for homogeneous turbulence. But how would one make meaningful comparisons when the turbulence is inhomogeneous? The results presented thus far indicate that even for the simple geometry and boundary conditions being considered in this study, a DNS with N^3 grid points would require a *minimum* of N^3+1 members in the ensemble to have enough degrees of freedom to satisfy the RRPA (assuming that it is valid for Navier-Stokes).

In the near future, even with computer speed and parallelization progressing at the current rate, it is highly unlikely that one will be able to include such a large number of realizations in the ensemble. Therefore, all comparisons between DNS data and a spectral model will have two sources of error, one arising from the limited number of realizations and the other from the particular closure scheme and assumptions inherent in the model. As was previously mentioned, all spectral models will have to assume that the RRPA is valid in order to make viable the number of computations per time step in updating the ensemble-averaged energy spectrum. The stern consequence is that even if one can construct rigorous spectral models for inhomogeneous turbulence (see Ref. [5] or [15], for example), the error due to having such a limited number of realizations for the DNS might overwhelm the error introduced by the model itself and in effect, make any comparison meaningless.

VI. CONCLUSIONS

This study has used DNS of both the Navier-Stokes and truncated Euler equations suitable for a rectangular channel flow with free slip, stress free walls to test a statistical assumption (the RRPA) involving second-order moments of the ensemble averaged spectral coefficients. It was demonstrated that simply to test this assumption in its broadest sense with an N^3 grid would actually require the inclusion of N^3+1 members in the ensemble. As a consequence of including fewer realizations, a distribution of $|\chi|$ values (the modulus of the normalized spectral covariance) results, which was shown to be both stationary in time and virtually free of spatial dependencies. Three ensembles consisting of 17 realizations were evolved in time (two updated from the Navier-Stokes equations and one from the Euler equation) with the difference between the two NS ensembles being that an orthogonalization procedure was either employed or not employed at $t=0$.

The main result is that the PDF of $|\chi|$ for the Euler system is identical to the PDF of $|\chi|$ created from an ensemble of random fields, while there are slight differences between the PDF from this random ensemble and the one resulting from the NS systems. Thus, viscosity is seen to play a role in

keeping the spectral coefficients from their most random distribution given the limited number of degrees of freedom present. More work needs to be done to ascertain whether the agreement between these PDFs improves or worsens as more members are included in the ensemble. It was also shown that as more random fields are generated, that the PDF of $|\chi|$ approaches a Dirac delta function at $|\chi|=0^+$, which is consistent with the RRPA. Equation (21) suggested that a correlation might exist between a mode and its reflection in the k_y direction. The apparent strong correlation at early times between these modes from the E1 ensemble was traced to the orthogonalization procedure used to generate the initial ensemble. Both the E2 and E3 ensembles did not exhibit such strong correlations at short times.

It may seem strange that we have tested the RRPA by considering the distribution of the modulus of χ, rather than utilizing the phase information. But what the RRPA is really asserting is that the phases of the products of any two independent spectral coefficients in *each realization* are uncorrelated with the phases of the same two modes in other realizations, so that the ensemble averaged product is identically zero. Therefore, the modulus of χ is the appropriate quantity to consider. Although not shown, the time history of the phasing of the spectral covariance has been computed and all three ensembles exhibit a uniform distribution between 0 and 2π. We have also discussed the difficulties that arise when comparing DNS results for inhomogeneous turbulence to those from a spectral model. It is not readily apparent how one will be able to separate out and quantify the error due to only evolving a limited number of realizations from the error incurred by the closure and other assumptions needed to form the model.

In addition, we showed that the statistics from the ensemble are markedly different from those of a particular realization. This strongly suggests the use of ensemble averages for the study of inhomogeneous turbulence. Whether or not this suggestion is warranted for homogeneous turbulence or turbulence which can be considered homogeneous in the axisymmetric directions for this channel flow will be the subject of a future study.

Finally, one may ask whether the RRPA would remain valid for a different geometry (i.e., flow in a pipe or flow over a sphere) with the same stress-free boundary conditions. As the equipartition argument for the energy (in the absence of kinetic helicity) remains valid, there is no reason why the RRPA should not hold for these more complicated inviscid flows. What would happen with the addition of viscosity is not clear at present. As only slight departures from the RRPA were observed for the rectangular channel flow with a finite viscosity, one might anticipate that the same result would occur once one considers the Navier-Stokes equations in cylindrical or spherical coordinates. Complex inhomogeneous flows such as Kelvin-Helmholtz could also be analyzed using this orthogonal decomposition, and DNS would provide a means of determining whether the RRPA is justified or whether additional couplings between spectral coefficients occur which then need to be included in the modeling. Provided that the number of additional couplings is small, these off-diagonal contributions could be incorporated into a spectral model without making it computationally prohibitive.

ACKNOWLEDGMENT

This work was supported by the U.S. Department of Energy LDRD Program under Project Nos. LDRD-97018 and LDRD-97601.

APPENDIX

A common strategy to ''augment'' the statistical sample size of turbulence simulations is to assume statistical homogeneity in the coordinate directions of the simulation which satisfy periodic boundary conditions. For example, if an ''ergodic hypothesis'' is invoked for a single numerical simulation of a stochastic system which employs a Fourier representation on a periodic mesh [16], one might then substitute the spatial average for the ensemble average based on the presumption that the ensemble is statistically homogeneous. However, the diagonality of spectra computed from a single simulation is a result of the orthogonality of the basis functions, and not a consequence of the statistical homogeneity of the field. For simplicity, we shall demonstrate this ''diagonality'' with a 1D example. The signal is represented as an N-length Fourier series

$$f(x)=\sum_{k=-N/2}^{N/2-1}\hat{f}(k)e^{-ikx}, \tag{A1}$$

and any displacement of x can be represented as a change in phase of the Fourier coefficient $\hat{f}(k)$;

$$\begin{aligned} f(x+\Delta_x)&=\sum_{k=-N/2}^{N/2-1}\hat{f}(k)e^{-ik(x+\Delta_x)}\\ &=\sum_{k=-N/2}^{N/2-1}[\hat{f}(k)e^{-ik\Delta_x}]e^{-ikx}\\ &=\sum_{k=-N/2}^{N/2-1}[\hat{f}_{\Delta_x}(k)]e^{-ikx}, \end{aligned} \tag{A2}$$

where $\hat{f}_{\Delta_x}(k)=\hat{f}_0(k)e^{-ik\Delta_x}$ is the displaced representation of the Fourier coefficient and $\hat{f}_0(k)=\hat{f}(k)$ is the undisplaced, or ''base'' representation of the coefficient. Note that $\hat{f}(k)\hat{f}(q)$ averaged over all (discrete) translations of the mesh $\Delta_x=n\delta_x$ is given by

$$\begin{aligned} \langle\hat{f}(k)\hat{f}(q)\rangle_x&=\frac{1}{N}\sum_{n=0}^{N-1}\hat{f}_{n\delta_x}(k)\hat{f}_{n\delta_x}(q)\\ &=\frac{1}{N}\sum_{n=0}^{N-1}\hat{f}(k)\hat{f}(q)e^{+i(k+q)n\delta_x}\\ &=\hat{f}(k)\hat{f}(q)\,\delta(k+q), \end{aligned} \tag{A3}$$

where $\langle\cdots\rangle_x$ denotes a spatial average and $\delta_x=2\pi/N$. Thus, we see that the spatial average ''diagonalizes'' as a consequence of the orthogonality of the basis functions over the domain. This diagonality is unrelated to the statistical diagonalization which would be associated with a statistically homogeneous ensemble of realizations which may, or may not be periodic. That is, the ''diagonality'' of the spatial average

does not imply that such a property is possessed by the ensemble. Indeed, it is undoubtedly a trivial proposition to construct a representation that is periodic yet possesses strong cross-phase correlations. Likewise, representation of a signal by a periodic basis function does not guarantee homogeneity (see Ref. [17]). Thus an individual simulation of a homogeneous turbulence may bear the same statistical relationship to a truly homogeneous (random-phase) ensemble that the inhomogeneous simulations described in this paper bear to the full restricted random phase ensemble.

[1] M. Lesieur, *Turbulence in Fluids*, 2nd ed. (Kluwer Academic, Boston, 1990).
[2] G. K. Batchelor, *The Theory of Homogeneous Turbulence*, 1st ed. (Cambridge University Press, Cambridge, 1953).
[3] D. C. Besnard, F. H. Harlow, R. M. Rauenzahn, and C. Zemach, Theor. Comput. Sci. **8**, 1 (1996).
[4] J. P. Bertoglio and D. Jeandel, *Turbulent Shear Flows 5*, 1st ed. (Springer-Verlag, Cambridge, 1998).
[5] L. Turner, LANL Unclassified Report No. LA-UR-96-3257, 1996.
[6] P. Y. Chou, Chin. J. Phys. **4**, 1 (1940).
[7] M. Millionshtchikov, Dokl. Akad. Nauk SSSR **32**, 615 (1941).
[8] R. H. Kraichnan, Phys. Fluids **7**, 1169 (1964).
[9] R. H. Kraichnan, J. Fluid Mech. **56**, 287 (1972).
[10] L. Turner, Ann. Phys. (N.Y.) **149**, 58 (1983).
[11] T. D. Lee, Q. Appl. Math. **10**, 69 (1952).
[12] R. H. Kraichnan, J. Fluid Mech. **59**, 745 (1973).
[13] S. Orszag, in *Fluid Dynamics*, edited by Balian Peube (Gordon and Breach Publishers, London, 1973), p. 235.
[14] W. Press, S. Teukolsky, W. Vellerling, and B. Flannery, *Numerical Recipes in Fortran*, 2nd ed. (Cambridge University Press, Cambridge, 1992).
[15] L. Turner, LANL Unclassified Report No. LA-UR-97-339, 1997.
[16] C. Canuto, M. Y. Hussaini, A. Quateroni, and T. A. Zang, *Spectral Methods in Fluid Mechanics*, 1st ed. (Springer-Verlag, New York, 1988).
[17] J. R. Chasnov, J. Fluid Mech. **342**, 335 (1997).